The Plant Cell, Vol. 25: 1274–1287, April 2013, www.plantcell.org

The Classical Arabinogalactan Protein AGP18 Mediates Megaspore Selection in *Arabidopsis*[W][OA]

Edgar Demesa-Arévalo and Jean-Philippe Vielle-Calzada[1]

Grupo de Desarrollo Reproductivo y Apomixis, Laboratorio Nacional de Genómica para la Biodiversidad y Departamento de Ingeniería Genética de Plantas, Cinvestav Irapuato CP36821 Guanajuato, Mexico

Female gametogenesis in most flowering plants depends on the predetermined selection of a single meiotically derived cell, as the three other megaspores die without further division or differentiation. Although in *Arabidopsis thaliana* the formation of the functional megaspore (FM) is crucial for the establishment of the gametophytic generation, the mechanisms that determine the specification and fate of haploid cells remain unknown. Here, we show that the classical arabinogalactan protein 18 (AGP18) exerts an active regulation over the selection and survival of megaspores in *Arabidopsis*. During meiosis, AGP18 is expressed in integumentary cells located in the abaxial region of the ovule. Overexpression of *AGP18* results in the abnormal maintenance of surviving megaspores that can acquire a FM identity but is not sufficient to induce FM differentiation before meiosis, indicating that AGP18 positively promotes the selection of viable megaspores. We also show that all four meiotically derived cells in the ovule of *Arabidopsis* are competent to differentiate into a gametic precursor and that the function of AGP18 is important for their selection and viability. Our results suggest an evolutionary role for arabinogalactan proteins in the acquisition of monospory and the developmental plasticity that is intrinsic to sexual reproduction in flowering plants.

INTRODUCTION

The life cycle of angiosperms is composed of the temporally predominant diploid sporophytic generation, and the haploid gametophytic generation that is ephemeral and composed of only a few cells differentiating within specialized reproductive organs. In a young ovule primordium, the establishment of the gametophytic phase initiates with the differentiation of a single subepidermal cell, the megaspore mother cell (MMC), that undergoes meiosis to generate four haploid products, the megaspores. Close to 70% of all angiosperms examined to date are monosporic (Huang and Russell, 1992; Friedman and Ryerson, 2009), since only one haploid cell, the functional megaspore (FM), is at the origin of the gametophytic lineage, and the three additional haploid products degenerate without differentiation or division. In *Arabidopsis thaliana*, the nucleus of the FM undergoes three mitotic divisions without cytokinesis, giving rise to eight haploid nuclei that undergo cellularization and differentiation to form the *Polygonum* type of female gametophyte, composed of an egg cell, two synergids, a binucleated central cell, and three antipodals (Maheshwari, 1950; Misra, 1962; Webb and Gunning, 1990; Reiser and Fischer, 1993; Yang et al., 2010). After fertilization by two sister sperm cells, the egg cell will give rise to the embryo, and the central cell to the endosperm.

[1] Address correspondence to vielle@ira.cinvestav.mx.
The author responsible for distribution of materials integral to the findings presented in this article in accordance with the policy described in the Instructions for Authors (www.plantcell.org) is: Jean-Philippe Vielle-Calzada (vielle@ira.cinvestav.mx).
[W] Online version contains Web-only data.
[OA] Open Access articles can be viewed online without a subscription.
www.plantcell.org/cgi/doi/10.1105/tpc.112.106237

Whereas most flowering plants are monosporic and only differentiate the most proximally located megaspore with respect to the longitudinal axis of the ovule primordium, many species differentiate a FM from a differently positioned megaspore, and many others incorporate more than one haploid product into female gametogenesis (Maheshwari, 1950; Kapil and Bhatnagar, 1981; Huang and Russell, 1992; Ebert and Greilhuber, 2005), indicating that the selection of functional meiotically derived cells is regulated by a modulated and flexible developmental pathway. Although it is well established that the differentiation of an FM is crucial for the establishment of the gametophytic phase, the genetic basis and molecular mechanisms that determine the specification and fate of haploid cells remain unknown. Several nonmutually exclusive hypotheses have been advanced to explain FM selection and survival in monosporic species. For instance, Bell (1996) suggested that the FM is selected by a positive survival or protective signal emitted from nucellus cells adjacent to the chalazal spore. Although several lines of evidence suggest that patterns of communication between the sporophyte and the gametophyte prevail during early ovule development in *Arabidopsis* (Robinson-Beers et al., 1992; Elliott et al., 1996; Klucher et al., 1996; Olmedo-Monfil et al., 2010; Bencivenga et al., 2011; Tucker et al., 2012), molecules trafficking from the nucellus to the chalazal megaspore have yet to be identified. Ultrastructural studies of premeiotic and meiotic ovules in *Arabidopsis* have uncovered the presence of numerous plasmodesmata at the MMC chalazal pole that could promote direct communication and signaling between the FM and adjacent sporophytic cells (Bajon et al., 1999). A second hypothesis favors the possibility that megaspore degeneration requires physical isolation resulting from the accumulation of callose in the wall of nonfunctional megaspores. Callose deposition

has been strictly correlated with selection of the FM in several species (Rodkiewicz, 1970; Noher de Halac and Harte, 1977), including *Arabidopsis* (Webb and Gunning, 1990) and maize (*Zea mays*; Russell, 1979). In the ovule of *Arabidopsis*, during metaphase I, callose accumulates uniformly in the MMC to subsequently mark transversal walls of the resulting meiotic tetrad and progressively become abundant in all walls of the degenerating megaspores after completion of meiosis. By contrast, callose is absent from all FM examined to date regardless of the position of the cell within the nucellar region of the ovule (Webb and Gunning, 1990), supporting the hypothesis of a physical isolation barrier determining the selection of functional meiotic products. Recent results showed that a sporophytic cytokinin signal has a role in the specification of the *Arabidopsis* FM (Cheng et al., 2013), without having an effect on the selection of the viable meiotic product. To date, *antikevorkian* is the only mutant of *Arabidopsis* that is affected in the selection of megaspores, as it forms multiple female gametophytes presumably originating from supernumerary surviving megaspores at a low frequency (Yang and Sundaresan, 2000); however, the corresponding locus has yet to be identified and characterized, and the genetic basis and molecular mechanisms that regulate megaspore selection and specification remain unknown.

Classical arabinogalactan proteins (AGPs) are an abundant class of highly glycosylated proteins attached to the plasma membrane of plants through a glycosylphosphotidylinositol (GPI) anchor (Youl et al., 1998; Borner et al., 2003; Ellis et al., 2010). Although their structural nature suggests that they could act as signaling molecules playing a flexible role of receptors or coreceptors in conjunction with the plant cell wall (Seifert and Roberts, 2007; Ellis et al., 2010; Zhang et al., 2011b), their molecular function and mechanisms of action are poorly elucidated. Initial studies using monoclonal antibodies raised against their carbohydrate residues determined that the patterns of AGP localization are highly dynamic during the sporophyte-to-gametophyte transition, suggesting that AGPs might represent molecular markers of a specific reproductive or vegetative lineage (Pennell and Roberts, 1990; Pennell et al., 1991, 1992; Coimbra et al., 2007). The functional characterization of classical AGPs has been impaired mainly by their structural complexity and the lack of specific antibodies against their proteic backbone (Tan et al., 2012). Although a specific role during reproductive development is usually attributed to possible tissue-specific posttranslational modifications, the cellular machinery involved in their complex and highly specific patterns of glycosylation remains elusive and hardly accessible in the ovule (Estévez et al., 2006; Velasquez et al., 2011).

Using a combination of enhancer detection tagging and RNA interference (RNAi) posttranscriptional silencing, we previously demonstrated that *AGP18*, a gene encoding a classical AGP of *Arabidopsis*, is essential for the initiation of female gametogenesis (Acosta-García and Vielle-Calzada, 2004). AGP18 RNAi individuals showing reduced or null AGP18 expression are sterile and exhibit normally differentiated ovules with FMs arrested before the first haploid mitotic division, indicating that AGP18 is necessary for the initiation of female gametogenesis. Like At-AGP17 and At-AGP19, the localization of AGP18 was confirmed to be at the plasma membrane by overexpression in vegetative cells (Zhang et al., 2011a); however, its localization in sporophytic or gametophytic cells of the developing ovule has not been determined. Although previous results open the possibility for AGP18 to promote cell functional acquisition during ovule development, the role of AGP18 and its exact mode of action during the control of early female gametogenesis have not been further investigated.

Here, we present a molecular dissection of the genomic regulatory region that drives *AGP18* expression and determines its pattern of protein localization in the developing ovule of *Arabidopsis*. We show that its distribution intersects the sporophytic–gametophytic transition, highlighting differences in transcriptional and translational regulation at the alternation of generations. We demonstrate that overexpression of *AGP18* in the ovule results in the abnormal maintenance of several surviving meiotically derived cells that acquire a FM identity but is not sufficient to induce FM identity before meiosis, indicating that AGP18 actively promotes the selection of viable megaspores at the end of megasporogenesis. Our findings indicate that classical AGPs are important for the establishment of prevalent developmental mechanisms that in flowering plants have favored the formation of a female gametophyte from consecutive divisions of a single meiotically derived cell.

RESULTS

AGP18 Is Transcriptionally Active in the Sporophyte during Megaspore Formation

To perform a functional dissection of the regulatory elements present in the intergenic region upstream of the *AGP18* coding region, we conducted a predictive analysis of the 1622-bp region that constitutes the *AGP18* upstream genomic region. The *cis*-elements were arbitrarily grouped in four regions, using the transcriptional initiation site (+1) as a reference for nucleotide location: (1) segment −1622 to −1217 contains elements linked to hormone regulation, such as an auxin response factor (ARF) binding motif (TGTCTC), a gibberellin response GAREAT (TAACAAR) box, and a drought response element core motif (RCCGAC) associated with the abscisic acid (ABA) response (Skriver et al., 1991; Yamaguchi-Shinozaki and Shinozaki, 1994; Ulmasov et al., 1995); (2) segment −1217 to −559 contains a CpG island and three copies of the C (A/T)8 G promoter motif CArG that binds proteins such as transcription factors of the MADS type or the floral repressor FLOWERING LOCUS C (Hepworth et al., 2002); (3) segment −559 to −162 contains two additional CArG motifs; and (4) the segment between −162 and the transcription starting site contains a TATA-box and Box II promoter motif (Le Gourrierec et al., 1999).

Based on this analysis, five distinct transcriptional fusions to the *uidA* (β-glucuronidase [GUS]) reporter gene were generated. Whereas the first two include the complete intergenic region with or without the 5′-untranslated region (UTR) AGP18 region (*proAGP18*$_{1622UTR}$*-GUS* and *proAGP18*$_{1622}$*-GUS*, respectively), the three others correspond to sequential 5′ deletions of the promoter at −1217, −559, and −162 bp (*proAGP18*$_{1217}$*-GUS*, *proAGP18*$_{559}$*-GUS*, and *proAGP18*$_{162}$*-GUS*, respectively; Figure 1). For each construct, at least five independent transformant lines

were analyzed and followed over two consecutive generations (with multiple individuals analyzed for each line and generation; see details in Methods). Consistent with previously reported results (Yang and Showalter, 2007), all constructs showed equivalent expression patterns in vegetative organs (see Supplemental Figure 1 online). By contrast, two distinct patterns were identified during ovule development. In multiple lines harboring *proAGP18*$_{1622UTR}$*-GUS*, *proAGP18*$_{1622}$*-GUS*, *proAGP18*$_{1217}$*-GUS*, or *proAGP18*$_{559}$*-GUS* (20 out of 27 transformant lines tested), reporter expression initiated at the end of megasporogenesis, prior

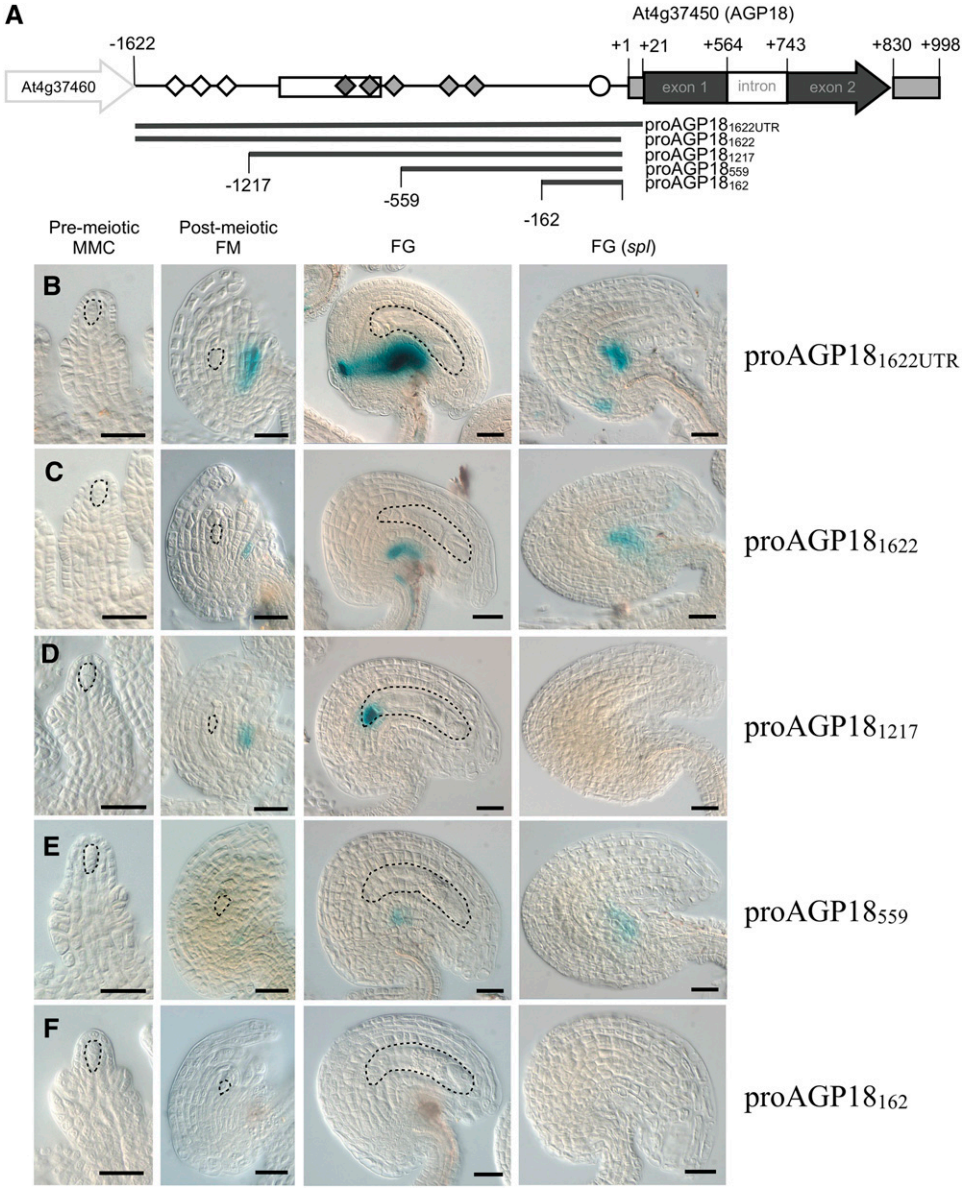

Figure 1. Molecular Dissection of the *AGP18* Regulatory Region.

(A) Diagram illustrating the structure of the *AGP18* locus and the genomic position of all five regulatory segments; coordinates are estimated by taking the *AGP18* transcription initiation site as a reference (+1). The regulatory region contains putative motifs for response to several phytohormones (white rhombus), a CpG island (rectangle), CArG boxes (gray rhombus), and a TATA-box (white circle).
(B) Pattern of GUS expression driven by *proAGP18*$_{1622UTR}$.
(C) Pattern of GUS expression driven by *proAGP18*$_{1622}$.
(D) Pattern of GUS expression driven by *proAGP18*$_{1217}$.
(E) Pattern of GUS expression driven by *proAGP18*$_{559}$.
(F) Pattern of GUS expression driven by *proAGP18*$_{162}$.
Dotted lines highlight the MMC, the FM, and the differentiated female gametophyte (FG). Bars = 20 μm.

to the first mitotic division of the FM, in a cluster of cells located at the base of the integuments, in the abaxial region of the ovule, and encompassing the external layer of internal integument and the internal layer of the external integument (Figures 1B to 1E). This pattern of expression expanded during megagametogenesis to form a ring of nucellar cells that covers the developing female gametophyte in the chalazal region. Lines harboring *proAGP18*$_{1217}$*-GUS* and *proAGP*$_{559}$*-GUS* showed weak sporophytic expression in the abaxial growing integuments; whereas transformants with *proAGP18*$_{1217}$*-GUS* showed consistent weak expression in the sporophyte but strong expression in the antipodals, lines harboring *proAGP18*$_{559}$*-GUS* showed stronger expression in the sporophyte but lacked expression in female gametophytic cells (Figures 1D and 1E). *proAGP18*$_{162}$*-GUS* did not show GUS expression in the ovule (Figure 1F). These results suggest that the −559 to −1 segment containing the CArG motifs controls the *AGP18* sporophytic expression pattern. They also suggest that in the absence of the −1622 to −1217 segment, the −1217 to −559 segment containing a CpG island negatively regulates the expression of *AGP18* in the sporophyte. Since the intensity of GUS staining is weaker in *proAGP18*$_{559}$*-GUS* than in the version including the full intergenic region, we conclude that elements driving quantitative expression are mainly present upstream of −559.

To confirm the nature of the observed expression patterns and determine if they depend on a possible sporophytic or gametophyte control, we crossed lines harboring each of all five constructs to individuals of the mutant *sporocyteless* (*spl*) that do not form a MMC and therefore lack the full gametophytic lineage (Schiefthaler et al., 1999; Yang et al., 1999). Despite the absence of a female gametophyte, all homozygous *spl* lines harboring *proAGP18*$_{1622UTR}$*-GUS*, *proAGP18*$_{1622}$*-GUS*, *proAGP18*$_{1217}$*-GUS*, and *proAGP18*$_{559}$*-GUS* maintained a reporter expression pattern in the sporophyte at weaker levels than the wild type, suggesting a weak genetic interaction between *AGP18* and *spl* or a partial gametophytic control of *AGP18* expression in the sporophyte (Figures 1B, 1C, and 1E). As expected, *proAGP18*$_{1217}$*-GUS* transformants that showed expression in the antipodals of wild-type ovules did not show GUS activity in *spl* individuals (Figure 1D), indicating that the establishment of the sporophytic pattern of *AGP18* expression is dependent on cues found within the sporophyte itself. Taken together, these results suggest that *AGP18* is transcriptionally regulated at two independent spatial and temporal domains: during early ovule development in integumentary (sporophytic) cells at the time of the sporophyte-to-gametophyte transition and in haploid gametophytic cells at the time of female gametophyte cellularization.

The Pattern of AGP18 Localization Intersects the Sporophyte-to-Gametophyte Transition

To gain insight into the role of AGP18 during gametophytic development, we determined the pattern of AGP18 localization in developing ovules. Regulatory regions *proAGP18*$_{1622}$ and *proAGP18*$_{1217}$ were selected to drive expression of chimeric versions of full-length *AGP18* fused to antigenic epitopes cMyc or 6XHis. Classical AGPs, such as AGP18, contain an N-terminal signal peptide that targets the propeptide to the endoplasmic reticulum (Chen et al., 1994; Du et al., 1994), and a C-terminal domain responsible for attaching the protein backbone to a GPI membrane anchor (Schultz et al., 1998; Youl et al., 1998; Sherrier et al., 1999; Schindelman et al., 2001; Borner et al., 2002; Sun et al., 2004); these features complicate the construction of antigenic fusions. To analyze the endogenous distribution of AGP18, antigenic epitopes were introduced downstream of the N-terminal signal peptide to favor the exposure of the epitope after potential peptide cleavage (Figure 2A). After selecting 35 stable *proAGP18*$_{1622}$*:cMyc-AGP18* and *proAGP18*$_{1217}$*:cMyc-AGP18* lines in the T1 generation, an anti-cMyc antibody was used to perform systematic immunolocalizations at all stages of ovule development. All stable T2 transformants used as reference lines for both type of constructs showed equivalent patterns of AGP18 localization. In premeiotic ovules, AGP18 was distributed uniformly in sporophytic cells and notably absent in the MMC; at the intracellular level, AGP18 was localized in the plasma membrane but also within cytoplasmic foci of sporophytic nucellar cells adjacent to the MMC (Figure 2B; see Supplemental Figure 2 online). After meiosis II, AGP18 was initially expressed in the FM at the time of its elongation (Figure 2C). The distribution of AGP18 in nucellar cells was polarized, with abundant expression in cellular edges adjacent to the FM (Figures 2C and 2D). In other sporophytic cells, AGP18 was often localized within cytoplasmic foci adjacent to their nucleus (Figure 2E). Since previously reported in situ hybridization (ISH) showed that AGP18 mRNA is localized in premeiotic cells of the developing ovule (Acosta-García and Vielle-Calzada, 2004), the localization of *AGP18* mRNA precedes the localization of the corresponding protein in the gametophytic lineage. In fully differentiated ovules, AGP18 was localized within the female gametophyte, in the central cell and the egg apparatus, but absent in the antipodals (Figures 2G and 2H). Additionally, AGP18 was localized in chalazally located nucellar cells that show reporter gene expression driven by the *proAGP18*$_{1622}$ promoter (Figure 2F). In summary, these results suggest that *AGP18* gene expression initiates in a cluster of sporophytic cells at stages encompassing megasporogenesis and FM differentiation.

Overexpression of *AGP18* Results in the Differentiation of Supernumerary Nucellar Cells

We previously demonstrated that *AGP18* is essential for the initiation of female gametogenesis following differentiation of the FM (Acosta-García and Vielle-Calzada, 2004); however, its pattern of transcriptional activity and protein localization suggests an earlier role during megasporogenesis. To investigate this possibility, we generated transgenic lines expressing *AGP18* under control of the cauliflower mosaic virus 35S promoter (CaMV35S) or of two previously analyzed *AGP18* endogenous regulatory regions, *pAGP18*$_{1622}$ and *pAGP18*$_{1217}$. The CaMV35S promoter has been shown to constitutively drive expression in sporophytic but not gametophytic cells of the ovule (Bechtold et al., 2000; Desfeux et al., 2000). A total of 95 individuals showing significantly reduced fertility compared with the wild type were found among all 216 independent T1 transformant lines analyzed (see Supplemental Tables 1 and 2 online), suggesting that overexpression of *AGP18* affects reproductive development. The percentage of unfertilized ovules in these lines ranged from 8 to 97%, and reduced fertility

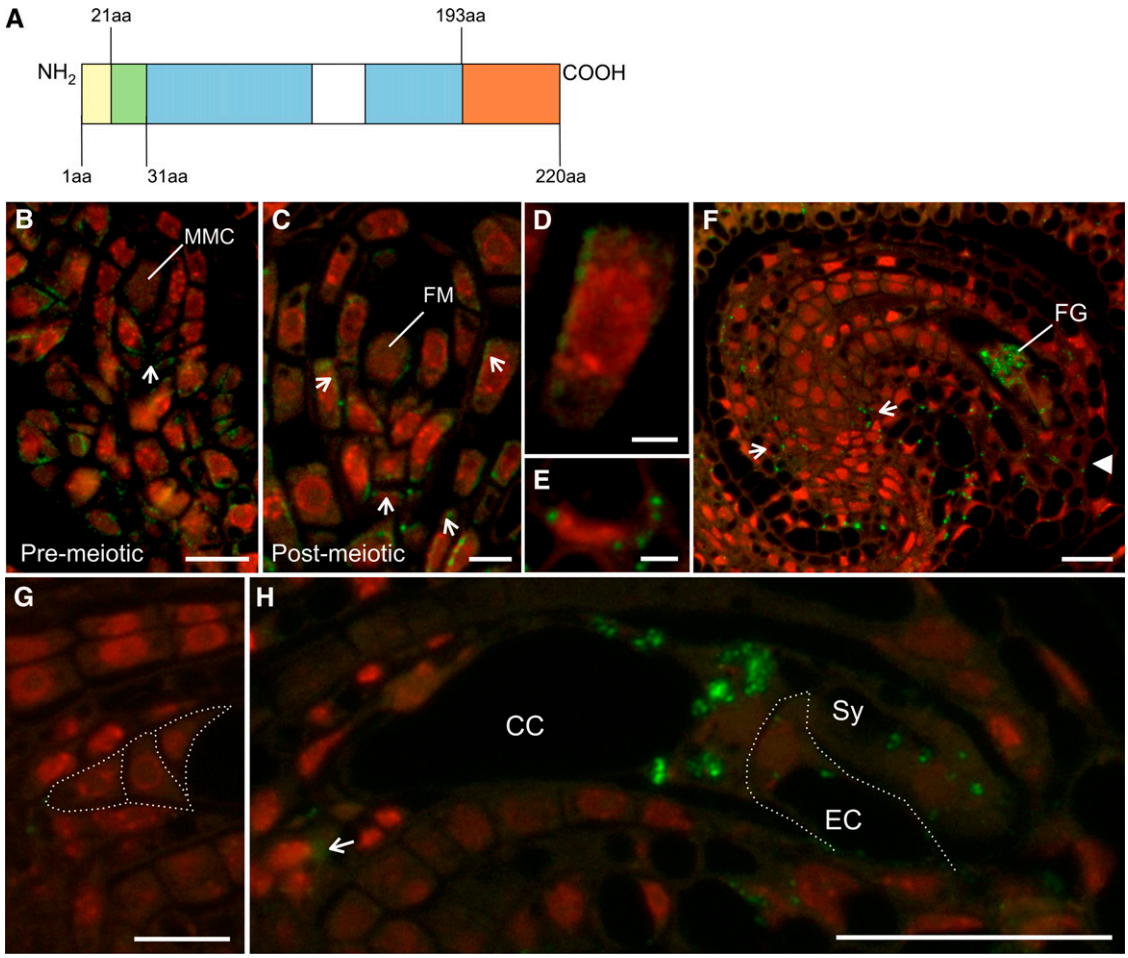

Figure 2. Localization of AGP18 during Ovule Development.

(A) In AGP18, an antigenic tag cMyc or 6XHis (green) was cloned between the signal peptide (yellow) and the Hyp-rich domain (blue); the lysine-rich domain (white) and the GPI anchoring domain (orange) are also highlighted; numbers indicate amino acid (aa) positions with respect to the initiation of the chimeric AGP18 protein sequence. All observations in **(B)** to **(H)** correspond to line *pAGP18*$_{1622}$:*cMyc-AGP18-10*.
(B) At premeiotic stages, AGP18 is localized in cytoplasmic foci (green) located the periphery of nucellar cells (arrow) but absent from the MMC.
(C) to **(E)** At postmeiotic stages, AGP18 is weakly expressed in the FM but abundantly localized in nucellar and integumentary cells (**[C]**, arrows, and **[D]**) and often in cytoplasmic domains adjacent to the nucleus of sporophytic cells **(E)**. **(D)** represents an enlargement of the region boxed in **(C)**.
(F) AGP18 localization in fully differentiated ovules containing a mature female gametophyte, sporophytic nucellar cells (arrows), and integumentary cells of the micropyle (arrowhead).
(G) AGP18 is not expressed in the antipodals (dotted lines).
(H) AGP18 is abundantly expressed in the central cell, the synergids, and the egg cell (dotted lines). The arrow shows expression in sporophytic cells of the chalaza.
Nuclei appear counterstained with 4',6-diamidino-2-phenylindole (red). CC, central cell; EC, egg cell; FG, female gametophyte; Sy, synergid. Bars = 10 μm in **(B)** and **(G)**, 5 μm in **(C)**, 2 μm in **(D)**, 3 μm in **(E)**, 15 μm in **(F)**, and 25 μm in **(H)**.

did not correlate with the nature of the regulatory region driving *AGP18* overexpression. To establish the cellular nature of the fertility defect, eight transformant lines showing high levels of sterility and harboring an *AGP18*-overexpressing transgene (either CaMV35S, *pAGP18*$_{1622}$, or *pAGP18*$_{1217}$) were selected for further analysis in the T2 generation. At fully differentiated stages of ovule development, 21.7 to 46.7% of ovules in each line showed a single FM-like cell arrested at 1-nuclear stage, 3 to 15.9% showed more than one differentiated cell reminiscent of the FM, and 4.7 to 17.9% showed a collapsed female gametophyte (see Supplemental Table 3 online); the rest of ovules in each line showed a normally cellularized female gametophyte undistinguishable from the wild type.

To determine the origin of the differentiated cells found arrested in mature ovules, we conducted a detailed cytological analysis of ovule development in four transformant lines, driving *AGP18* overexpression with either CaMV35S (two lines), *pAGP18*$_{1622}$ (one line), or *pAGP18*$_{1217}$ (one line). Results from this analysis are

illustrated in Figure 3 and Table 1. At premeiotic stages, overexpression of *AGP18* did not result in phenotypes distinguishable from the wild type (Figures 3A and 3B; see Supplemental Figure 3 online). At the end of meiosis, most wild-type ovules showed a linear tetrad that included three degenerated megaspores and a FM located at the most proximal position with respect to the placental attachment of the ovule to the gynoecia (Figures 3C to 3E; see Supplemental Figure 3 online); however, at a lower frequency of 9.1%, wild-type ovules showed noncanonical T-shape configurations in which the three degenerated megaspores

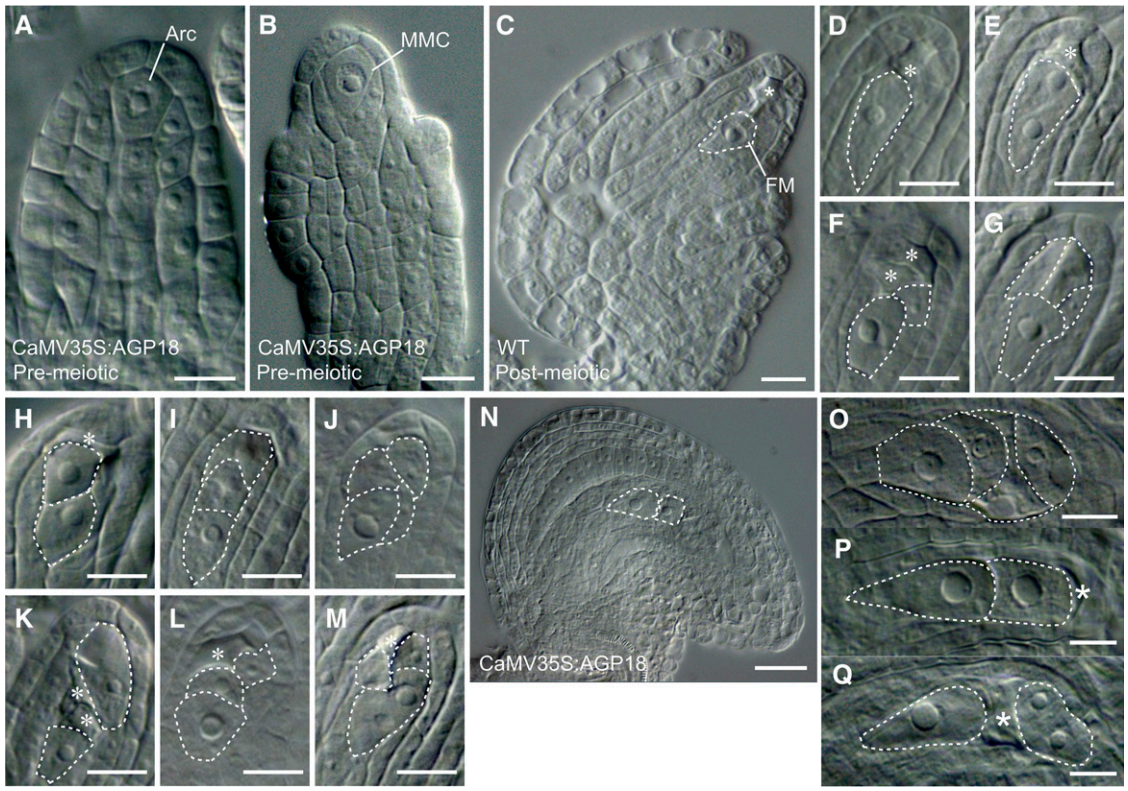

Figure 3. Megaspore Formation in Wild-Type and *AGP18*-Overexpressing Lines.

(A) Premeiotic ovule in a *CaMV35S:AGP18*-overexpressing line showing a single archeosporal cell (Arc) in the subepidermal layer.
(B) Premeiotic ovule in a *CaMV35S:AGP18*-overexpressing line showing a single MMC.
(C) Postmeiotic wild-type (WT) ovule showing a single surviving megaspore and the FM.
(D) Postmeiotic wild-type ovule showing an enlarged FM before division and the remnants of a degenerated megaspore.
(E) Postmeiotic wild-type ovule showing a 2-nuclear female gametophyte adjacent to the degenerated megaspores.
(F) Postmeiotic wild-type ovule showing a noncanonical tetrad configuration, with only two degenerated megaspores aligned to the FM, and a third one outside the linear alignment.
(G) Postmeiotic wild-type ovule showing a noncanonical T-shaped configuration, with three degenerating megaspores transversally aligned with respect to the ovule's longitudinal axis.
(H) Postmeiotic ovule in a *CaMV35S:AGP18*-overexpressing line showing two adjacent surviving megaspores (dashed) and one degenerated megaspore.
(I) Postmeiotic ovule in a *CaMV35S:AGP18*-overexpressing line showing three adjacent surviving megaspores.
(J) Postmeiotic ovule in a *CaMV35S:AGP18*-overexpressing line showing surviving megaspores in a noncanonical configuration.
(K) Postmeiotic ovule in a *CaMV35S:AGP18*-overexpressing line showing two surviving megaspores separated by two degenerated megaspores.
(L) Postmeiotic ovule in a *CaMV35S:AGP18*-overexpressing line showing three surviving megaspores in noncanonical configuration.
(M) Postmeiotic ovule in a *CaMV35S:AGP18*-overexpressing line showing a surviving megaspore that has undergone a nuclear division, adjacent to additional surviving megaspores.
(N) Fully differentiated ovule in *CaMV35S:AGP18*-overexpressing line showing two surviving megaspores.
(O) Fully differentiated ovule in a *CaMV35S:AGP18*-overexpressing line showing four surviving megaspores.
(P) Fully differentiated ovule of a *pAGP18*$_{1622}$*:AGP18*-overexpressing line showing a phenotype equivalent to **(H)**.
(Q) Fully differentiated ovule in a *pAGP18*$_{1217}$*:AGP18*-overexpressing line showing a phenotype similar to **(K)** and **(M)**.
Observations correspond to *CaMV35S:cMyc-AGP18-19*, *pAGP18*$_{1217}$*:cMyc-AGP18-12*, and *pAGP18*$_{1622}$*:cMyc-AGP18-09* (see Supplemental Table 3 online for details). Surviving megaspores are outlined by a dashed line and distinguishable degenerated megaspores by an asterisk. Bars = 10 μm in **(A)** to **(M)** and **(O)** to **(Q)** and 25 μm in **(N)**.

Table 1. Quantitative Analysis of Extranumerary Cells Present in Ovules at the End of Megasporogenesis

Genotype	Linear Tetrad	Noncanonical Tetrad	Extranumerary Surviving Cells
CaMV35S:cMyc-AGP18-19-T_2	164 (67.2%)	22 (9%)	58 (23.8%)[a]
CaMV35S:AGP18-10-T_2	268 (71.1%)	42 (11.1%)	67 (17.8%)[b]
Wild type	239 (87.2%)	25 (9.1%)	10 (3.6%)

[a] $\chi^2 = 285.96 > \chi^2_{0.05[1]} = 3.84$.
[b] $\chi^2 = 220.62 > \chi^2_{0.05[1]} = 3.84$.

did not align linearly but transversally with respect to the ovule's longitudinal axis (Figures 3F and 3G). By contrast, *CaMV35S*:*AGP18* transformants for both lines analyzed showed 17.8 and 23.8% of developing ovules containing extranumerary cells, reminiscent of surviving haploid products at the end of megasporogenesis (Table 1, Figures 3H to 3M), a higher frequency compared with the equivalent estimation conducted in fully differentiated ovules (Table 1; see Supplemental Table 3 online). In some cases, two or more aligned cells were distinguishable within the young nucellar tissue at locations usually occupied by degenerated megaspores (Figures 3H and 3I); in other cases, cells were organized in noncanonical configurations reminiscent of T-shape tetrads (Figure 3J), either adjacent or separated by at least one degenerated megaspore (Figures 3K and 3L), and with at least one differentiated cell having undergone an additional nuclear division (Figure 3M). Fully differentiated ovules contained either arrested differentiated cells (Figures 3N to 3Q) or cellularized female gametophytes undistinguishable from those of the wild type. In all cases, ovules of *CaMV35S:AGP18* transformants contained a maximum of four surviving cells reminiscent of haploid products, suggesting that these cells are the result of a single meiotic event occurring in the ovule. Because abnormal phenotypes could be related to the molecular nature of the selected promoter, or to previously reported semisterility defects caused by T-DNA chromosomal rearrangements (Ray et al., 1997; Curtis et al., 2009), we analyzed a group of transgenic lines harboring an empty construct that only included the CaMV35S regulatory region devoid of the *AGP18* gene. Among nine independent transgenic lines cytologically analyzed, none showed sterility defects at frequencies significantly different to the wild type ($\chi^2_{obs.} < \chi^2_{0.05[1]} = 3.84$ for all nine lines) nor did any show ovules containing extranumerary differentiated cells (see Supplemental Tables 2 and 3 online), indicating that the abnormal phenotypes previously described are caused by the overexpression of *AGP18*. Taken together, these results suggest that *AGP18* is involved in megaspore selection and survival during early female gametogenesis. Since extranumerary cells are observed at lower frequencies in fully differentiated ovules compared with the early stages of gametogenesis, we propose that differentiated cells found in lines overexpressing AGP18 are often reabsorbed during nucellar growth and expansion as a consequence of the defect during megasporogenesis, often giving rise to an arrested or collapsed female gametophyte.

Supernumerary Cells in Ovules Overexpressing *AGP18* Are of Meiotic Origin and Can Acquire an FM Identity

To determine if the supernumerary cells observed in ovules overexpressing *AGP18* are indeed of meiotic origin, we monitored the expression of the *Arabidopsis* homolog of *DISRUPTION OF MEIOTIC CONTROL1* (At-*DMC1*) by crossing a *pAtDMC1-GUS* reporter line to the *CaMV35S:AGP18* lines. At-*DMC1* is a meiosis-specific gene essential for DNA strand exchange between homologous chromosomes (Klimyuk and Jones, 1997; Couteau et al., 1999). In wild-type premeiotic ovules, the expression of *pAtDMC1-GUS* was restricted to the MMC (Figure 4A); following meiosis, GUS was expressed in the three degenerating megaspores but not in the FM (Figure 4B), as previously reported (Agashe et al., 2002). In ovules of *CaMV35S:AGP18* transformants, *pAtDMC1-GUS* was expressed in the MMC, suggesting that MMC fate is correctly defined. During meiosis but before differentiation of the FM, expression of *pAtDMC1-GUS* was invariably restricted to no more than three surviving cells in the nucellar tissue ($n = 184$; Figures 4C and 4D), suggesting that supernumerary cells are indeed derived from a single meiotic division and that a single meiotic division occurs in the ovule. To determine if at the end of meiosis supernumerary cells acquire a FM identity, we crossed *CaMV35S:AGP18* lines to transformants containing the *pFM2-GUS* translational reporter construct (Olmedo-Monfil et al., 2010), which is activated specifically upon FM specification and absent in the MMC and degenerating megaspores (Figures 4E and 4F). At subsequent stages, *pFM2-GUS* expression is maintained in the developing and fully cellularized female gametophyte (Figure 4I). Whereas premeiotic ovules overexpressing *AGP18* did not show changes in the pattern of GUS expression compared with *pFM2-GUS* transformants, postmeiotic ovules frequently exhibited two or more cells showing GUS expression (Figure 4G). In some cases, all four meiotic products showed GUS expression (Figure 4H), confirming that several meiotically derived cells survive and acquire a FM identity. At subsequent developmental stages, 5.3% ($n = 1061$) of fully differentiated ovules showed more than one FM-like cell expressing GUS, rather than a cellularized female gametophyte (Figure 4K; see Supplemental Table 3 online), whereas 46.7% contained a single FM (Figure 4J) and 38.2% showed a cellularized female gametophyte. Taken together, this evidence indicates that the overexpression of *AGP18* results in a single meiotic division with survival of more than one meiotically derived megaspore having the potential to acquire a FM identity.

AGP18 Is Required for Selection of a Viable Megaspore but Not Sufficient for Its Specification

Immunolocalizations showed that AGP18 is expressed in the MMC of *CaMV35S:AGP18* transformants (Figures 5A and 5B), confirming that transgenic expression occurs in sporophytic cells, including the MMC; however, *pFM2*-driven expression of *GUS* was absent in the MMC of these transformants, suggesting

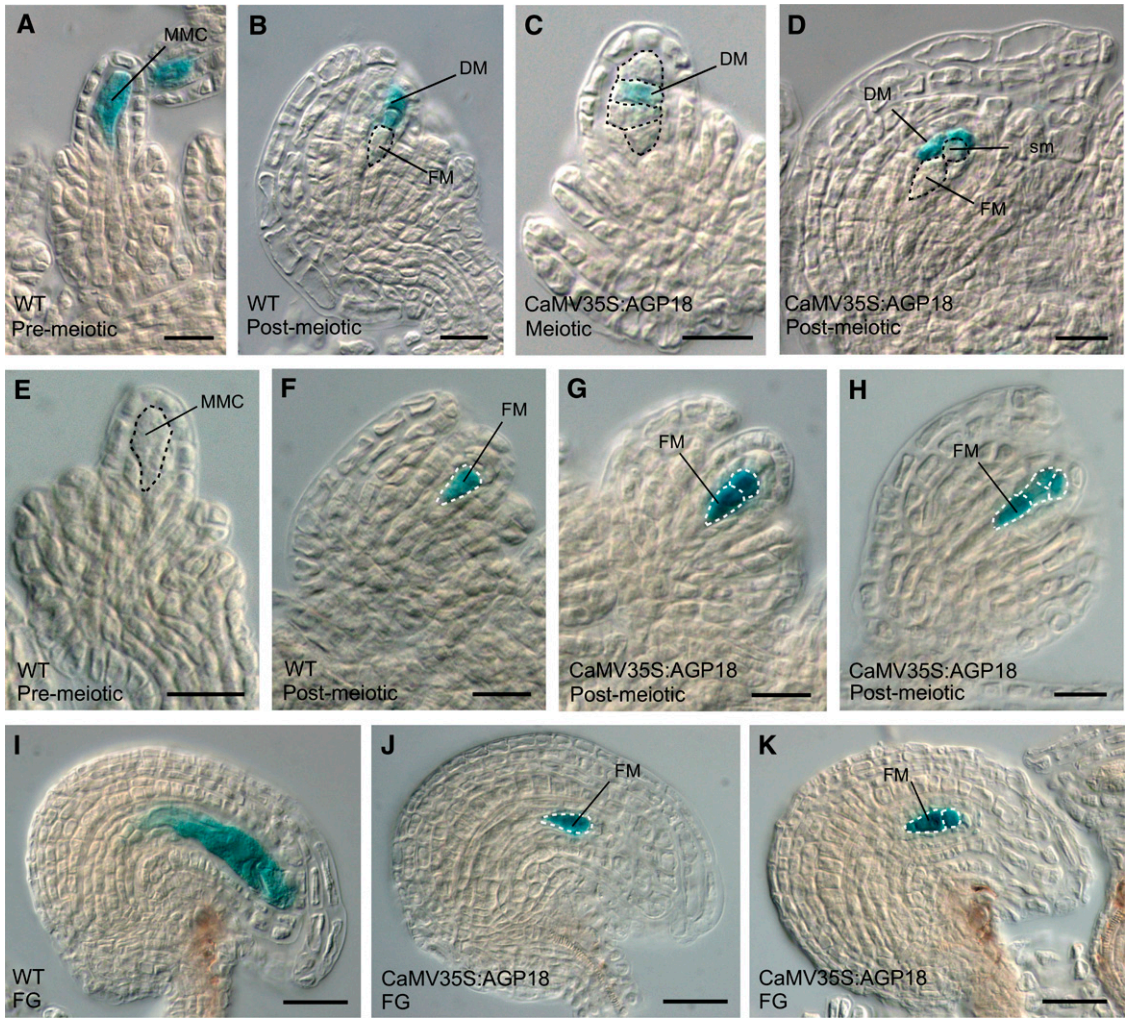

Figure 4. Extranumerary Cells in the Ovule of *AGP18*-Overexpressing Lines Are Meiotic Products That Acquire an FM Identity.

(A) Meiotic wild-type (WT) ovule showing expression of the *pAtDMC1-GUS* marker in the MMC.
(B) Postmeiotic wild-type ovule showing expression of the *pAtDMC1-GUS* marker only in the degenerating megaspores.
(C) Postmeiotic ovule in a *CaMV35S:AGP18*-overexpressing line showing absence of expression of the *pAtDMC1-GUS* marker in three out of four megaspores organized in a linear configuration.
(D) Postmeiotic ovule in a *CaMV35S:AGP18*-overexpressing line showing absence of expression of the *pAtDMC1-GUS* marker in two out of four surviving megaspores (sm) organized in a nonlinear configuration.
(E) Premeiotic ovule in a *pFM2-GUS* transformant showing absence of GUS expression in the MMC.
(F) Postmeiotic ovule in a *pFM2-GUS* transformant line showing GUS expression in the FM.
(G) Postmeiotic ovule in a *CaMV35S:AGP18*-overexpressing line showing GUS expression in two adjacent surviving megaspores.
(H) Postmeiotic ovule in a *CaMV35S:AGP18*-overexpressing line showing expression of the *pFM2-GUS* marker in all meiotically derived megaspores.
(I) Fully differentiated ovule showing expression of the *pFM2-GUS* marker in the female gametophyte.
(J) Fully differentiated ovule in a *CaMV35S:AGP18*-overexpressing line showing expression of the *pFM2-GUS* marker in a surviving megaspore.
(K) Fully differentiated ovule in a *CaMV35S:AGP18*-overexpressing line showing expression of the *pFM2-GUS* marker in two adjacent megaspores.
All crosses performed with *CaMV35S:cMyc-AGP18-19* (see Supplemental Table 3 for details). DM, degenerated megaspore. Megaspores are outlined by a dashed line. Bars = 15 μm in **(A)** to **(H)** and 25 μm in **(I)** to **(K)**.

that either *AGP18* expression is not sufficient to induce FM specification in the MMC or that posttranslational modifications required for *AGP18*-dependent FM specification do not take place in the MMC. To address these possibilities, we compared the localization of the AGP-related sugar epitope recognized by JIM13 in ovules of *CaMV35S:AGP18* and wild-type plants. JIM13 is a monoclonal antibody raised against carbohydrate residues acquired by some AGPs after posttranslational modifications, as previously shown in several flowering plant species that include *Arabidopsis* (Yates et al., 1996; Coimbra et al., 2007). In wild-type ovules, JIM13 is not detected during premeiotic or meiotic stages (Figure 5D). JIM13 is initially localized

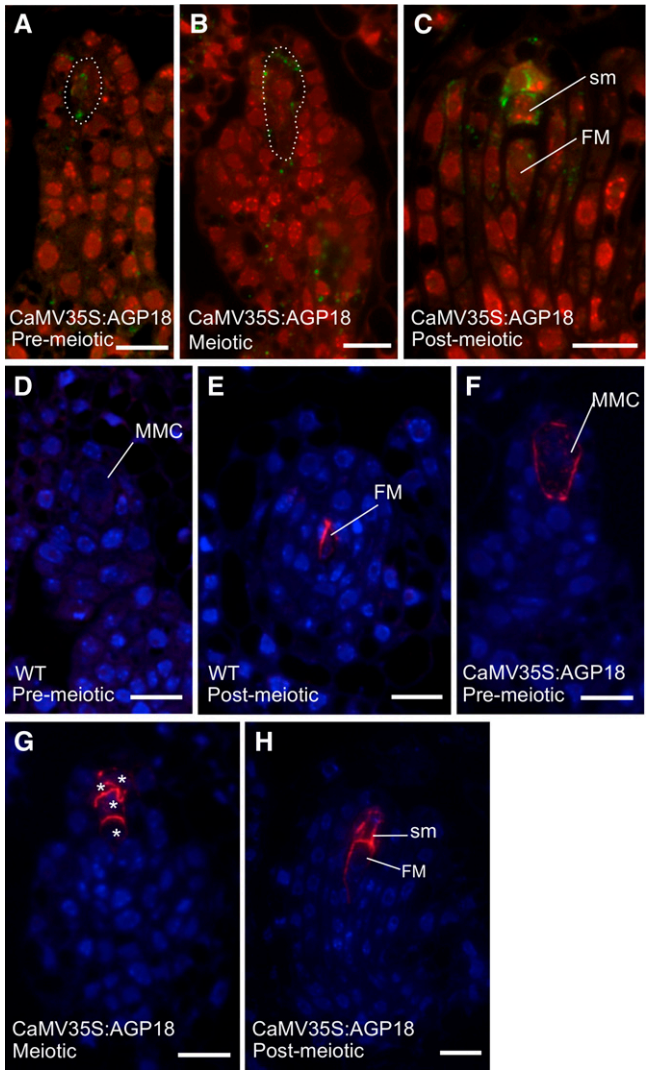

Figure 5. AGP18 Is Required for Selection of a Viable Megaspore but Not Sufficient for Its Specification.

(A) Premeiotic ovule in a *CaMV35S:AGP18* transformant line showing AGP18 expression in the MMC.
(B) Meiotic ovule in a *CaMV35S:AGP18* transformant line showing AGP18 expression in an enlarged MMC undergoing meiosis.
(C) Postmeiotic ovule in a *CaMV35S:AGP18* transformant line showing AGP18 expression in surviving megaspores.
(D) Premeiotic wild-type (WT) ovule showing absence of JIM13 localization.
(E) Postmeiotic wild-type ovule showing localization of JIM13 in the FM.
(F) Premeiotic ovule in a *CaMV35S:AGP*18-overexpressing line showing localization of JIM13 at the surface of the MMC.
(G) Meiotic ovule in a *CaMV35S:AGP*18-overexpressing line showing localization of JIM13 at the surface of the resulting megaspores (asterisks).
(H) Postmeiotic ovule in a *CaMV35S:AGP*18-overexpressing line showing localization of JIM13 at the surface of the FM and additional surviving megaspores.
All observations correspond to *CaMV35S:cMyc-AGP18-19*. sm, surviving megaspore. The MMC in **(A)** and **(B)** is outlined by a dashed line. Bars = 10 μm.

in the FM and subsequently in all cells of the developing female gametophyte (Figure 5E; see Supplemental Figure 4 online), confirming that the specific AGPs carbohydrate residues recognized by JIM13 are molecular markers of the gametophytic lineage. In wild-type ovules, our previous immunolocalizations show that AGP18 is expressed in sporophytic nucellar cells that do not exhibit JIM13 localization (Figures 2C and 5E). By contrast, in ovules of *CaMV35S:AGP18* transformants, JIM13 is ectopically localized in walls of the MMC and the four meiotically derived megaspores (Figures 5F and 5G) and, following meiosis, in all surviving megaspores (Figure 5H). In fully differentiated ovules, JIM13 is localized in arrested gametophytic cells but also in dorsal sporophytic cells that do not show localization of JIM13 in the wild type (see Supplemental Figure 4 online). This spatial and temporal pattern is equivalent to the pattern of AGP18 localization in ovules of *CaMV35S:AGP18* plants (Figures 5A to 5C), strongly suggesting that sugar residues recognized by JIM13 are present in AGP18 but that these residues are acquired by posttranslational modifications that initially occur only in the FM. They also suggest that neither AGP18 expression nor FM-specific posttranslational modifications are sufficient to shift MMC to FM identity.

DISCUSSION

We have found that the classical arabinogalactan protein AGP18 positively regulates the selection of megaspores at the end of megasporogenesis in *Arabidopsis*. At stages encompassing megasporogenesis, upstream regulatory regions drive initial *AGP18* transcription in a cluster of integumentary cells in the abaxial region of the ovule. Although additional regulatory elements located in the coding or 3′-UTR could also influence the pattern of *AGP18* activity, our results suggest that the *AGP18* transcript could be transported to act in the developing nucellus during megasporogenesis. In agreement with previous results showing that silencing of *AGP18* caused defects affecting the initiation of female gametogenesis by restricting the expansion and nuclear division of the FM (Acosta-García and Vielle-Calzada, 2004), sporophytic overexpression of *AGP18* results in reduced fertility and survival of one or multiple meiotic products, suggesting that *AGP18* promotes megaspore viability in the developing ovule.

A molecular dissection of the *AGP18* upstream region revealed that the expression of *AGP18* responds to molecular cues contained within regulatory elements. In addition to five CArG boxes predicted to bind MADS box transcription factors, the *AGP18* regulatory region contains auxin, gibberellin, and ABA response elements that suggest a hormonal control of *AGP18* transcription in the developing abaxial integumentary cells. Auxins are synthesized specifically in maternal sporophytic tissue during megasporogenesis, and mutants affected in auxin biosynthesis are defective in the establishment of the gametophytic phase (Stepanova et al., 2008; Pagnussat et al., 2009; Bencivenga et al., 2011). *AGP18* expression is induced by natural auxin indole-3-acetic acid in diverse *Arabidopsis* ecotypes (Delker et al., 2010) and repressed by ABA (Zhang et al., 2011a), consistent with the observed overexpression of *AGP18* mRNA in the ABA signaling double mutant *agb1 gpa1*, which is

defective in proteins GTP BINDING PROTEIN BETA1 (AGB1) and G PROTEIN ALPHA SUBUNIT1 (GPA1; Hruz et al., 2008; Pandey et al., 2010). Our results extend these findings by showing that hormone-related response elements are necessary for proper sporophytic expression of *AGP18* during megasporogenesis. By contrast, genomic elements driving specific transcriptional activation in the female gametophyte are located within a CpG island associated with methylation-dependent repetitive DNA silencing in *Arabidopsis* (Law and Jacobsen, 2010), suggesting that epigenetic mechanisms regulate *AGP18* expression in the female gametophyte, either directly through positive activation of the CpG island or indirectly through the regulation of the contained CArG boxes recruiting activating or repressing transcription factors. This CpG island does not differentially regulate *AGP18* expression in vegetative tissues, as the pattern of reporter gene expression was equivalent for all constructs analyzed.

While AGP18 protein is absent from the MMC, ISH showed that *AGP18* mRNA is ubiquitously localized in the apical region of the ovule primordium, including the MMC (Acosta-García and Vielle-Calzada, 2004), suggesting that *AGP18* mRNA translation is specifically repressed within the MMC. Cell-specific transcriptional analysis of laser-capture cells highlighted the importance of translational control factors acting in the MMC (Schmidt et al., 2011); however, our immunolocalization experiments in *CAMV35S:AGP18* lines showed that the MMC is competent for *AGP18* translation (Figures 5A and 5B), suggesting that the translational control of *AGP18* is likely based on transcript abundance rather than on molecular repression. This type of effect could also explain the incomplete penetrance of both RNAi silencing and *AGP18* overexpression defects in the ovule by mechanisms similar to those prevailing in *Caenorhabditis elegans*, in which incompletely penetrant mutant phenotypes are a consequence of a threshold in the expression of cell identity genes (Raj et al., 2010). Although the MMC appears to possess all the translational and posttranslational machinery required for AGP18 expression, the presence of this protein is not sufficient to switch the fate of a MMC to a FM in the absence of meiosis. In addition to previous results showing that gametophytic defects found in *AGP18-RNAi* lines are sporophytically controlled, the sporophytic nature of the *AGP18* mRNA pattern of expression is supported by crosses to *spl*, in which the absence of the female gametophyte does not modify reporter expression of *proAGP18*:*GUS* lines, and also by large-scale transcriptional analysis confirming that *AGP18* transcripts are present in both sporophytic and gametophytic cells (Sánchez-León et al., 2012). Based on the pattern of JIM13 localization, our results also suggest that AGP18 undergoes specific posttranslational glycosylations that initially occur only in the FM and not in adjacent nucellar cells. These results could imply that the acquisition of posttranslational modifications is specific to the gametophytic lineage, in agreement with a previous hypothesis that emphasized their importance for establishing transitions between a sporophyte and a gametophyte (Pennell and Roberts, 1990; Pennell et al., 1992). Whereas ISH experiments showed localization of *AGP18* mRNA in the egg apparatus and the antipodals but not in the central cell (Acosta-García and Vielle-Calzada, 2004), our results indicate that AGP18 is abundant in the central cell and egg apparatus but not in the antipodals. A large-scale transcriptional analysis of laser-capture microdissected gametophytic cells showed that *AGP18* transcripts are detected at low frequencies in the central cell (Wuest et al., 2010; Schmidt et al., 2011), suggesting that the sensitivity of ISH experiments was below the threshold of *AGP18* transcript detection in the female gametophyte or that *AGP18* mRNA can be transported to the central cell from the egg apparatus or the sporophyte. The absence of AGP18 in the antipodals suggests the existence of posttranscriptional regulation mechanisms in these cells or the absence of the translational and posttranslational machinery required for AGP18 protein expression.

Insertional lines harboring T-DNA or transposon elements within the regulatory or coding region of *AGP18* are unusually rare, suggesting that complete loss-of-function alleles are gametophytic lethal. The only two reported insertional lines available did not show obvious defects during either vegetative or reproductive development and do not show differences in the levels of *AGP18* expression compared with the wild type (SALK_117268, located at +820; and GT6565, at +871; Yang and Showalter, 2007). Although abnormal survival of meiotically derived megaspores has been reported for the *Arabidopsis* mutant *antikevorkian* at a presumed frequency of ~10% (Yang and Sundaresan, 2000; Tucker and Koltunow, 2009), its molecular function remains unknown. The variable number of differentiated megaspores found in ovules of *AGP18* overexpressing lines suggests that AGP18 could play a role in mediating some of the signaling pathways involved in determining megaspore fate following meiosis. In addition to megaspore degeneration and reabsorption during gametogenesis, the relatively low frequency at which multiple megaspores prevail could imply that several functionally redundant and nonexclusive regulatory pathways ensure a tight control over selection of a single FM in *Arabidopsis*. Although *AGP17* and *AGP19* are also expressed in the developing gynoecium of *Arabidopsis* (Acosta-García and Vielle-Calzada, 2004), a possible redundant function of *AGP18* with these closely related genes encoding AGPs remains to be investigated, although the scarcity of insertions in AGP18 suggests a nonredundant role for these proteins in the female gametophyte. Recently, cytokinin signaling has been implicated in the specification but not the selection of the *Arabidopsis* FM (Cheng et al., 2013), and previous results showed that processes involving protease activity (Chen et al., 2008), calcium concentration (Qiu et al., 2008), and callose deposition (Rodkiewicz, 1970; Webb and Gunning, 1990) are associated with megaspore degeneration, although their role is not understood. Determining if AGP18 mediates megaspore selection through regulatory controls that include some of these processes will require additional studies.

The role of AGPs of the AGP18 type might represent a significant step in establishing the reproductive mechanisms that prevail during megasporogenesis. Monospory (i.e., the formation of a female gametophyte from consecutive divisions of the most chalazally located megaspore) (Maheshwari, 1950; Misra, 1962; Webb and Gunning, 1990) is largely dominant among angiosperms; however, other alternatives, such as bispory and tetraspory, in which more than one meiotic product participates in gametogenesis, are also commonly found in multiple families

(Maheshwari, 1950; Kapil and Bhatnagar, 1981; Huang and Russell, 1992). Among monosporic species, several show developmental variants in which the FM is not the most chalazally located meiotic product (Maheshwari, 1950). By limiting competition for resource allocation and space, monospory is perceived as an evolutionary acquisition that prevents the formation of multiple female gametophytes within a single ovule, a feature more commonly found within ancient angiosperms (Bachelier and Friedman, 2011). Our findings open the possibility for investigating the evolutionary role that classical AGPs could have played for the acquisition of the developmental plasticity that is intrinsic to sexual reproduction in flowering plants.

METHODS

Plant Material and Growth Conditions

Wild-type plants, transgenic pFM2-GUS, and pAtDMC1-GUS are all in Columbia ecotype, whereas *spl* is in the Landsberg *erecta* background. Seeds were surface sterilized with 100% ethanol or with chlorine gas and germinated under stable long-day (16 h light/8 h dark) conditions in Murashige and Skoog (MS) medium at 22°C. Seedlings were planted and grown under controlled greenhouse conditions (24°C).

Generation and Analysis of *proAGP18*:*GUS* Transformants

The prediction of *cis*-elements in the intergenic region upstream of *AGP18* (At4g37450) was performed using Athena software (http://www.bioinformatics2.wsu.edu/Athena; O'Connor et al., 2005). Transcriptional fusions were generated by amplifying different segments of the *AGP18* intergenic regulatory region using the following primer combinations (see Supplemental Table 4 online): 1SpAGP18/5ASUTRpAGP18 (1643 bp), 1SpAGP18/1ASpAGP18 (1607 bp), 2SpAGP18/1ASpAGP18 (1202 bp), 3SpAGP18/1ASpAGP18 (544 bp), and 4SpAGP18/1ASpAGP18 (147 bp). Amplicons were cloned in pCR-TOPO 2.1 (Invitrogen) and digested with *Hin*dIII and *Xho*I. DNA fragments were cloned into pBI101.2 (Jefferson et al., 1987) to generate transcriptional fusions with the reporter gene *uid*A (GUS). Resulting pAGP18:GUS plasmids were transformed into *Agrobacterium tumefaciens* strain GV 2260 (McBride and Summerfelt, 1990) and subsequently into *Arabidopsis thaliana* Columbia-0 by floral dipping as previously described (Clough and Bent, 1998). Both T1 and T2 seeds obtained were germinated in MS medium containing kanamycin (50 μg mL^{-1}). For constructs harboring an endogenous promoter, kanamycin-resistant individuals (T1 and T2) were confirmed as transformants by conducting PCR using the pBI101-S/GUS-AS3 primer combination to amplify a pAGP18 fragment. In each case, at least five independent T1 and T2 lines were cytologically analyzed by quantifying phenotypes in at least five individuals per line. All primer sequences are described in Supplemental Table 4 online.

Generation of Overexpression and Antigenic Tagged Transformants

Total RNA was isolated using Trizol (Invitrogen) from wild-type inflorescences that were ground in liquid nitrogen. Approximately 5 μg of total RNA was treated with 5 units of RNase-free DNase (Boehringer-Mannheim) in 1× DNase buffer (Invitrogen) containing 20 mM $MgCl_2$; after 15 min at room temperature, reactions were heat inactivated at 65°C for 10 min. RNA was reverse transcribed using 20 pmol of an oligo(dT) primer (Sigma-Aldrich) in a 50-μL reaction containing 1× RT-PCR buffer (Invitrogen), 3 mM $MgCl_2$, 0.5 mM deoxynucleotide triphosphate (dNTP), 2.6 mM DTT, and 200 units of Superscript II reverse transcriptase (Invitrogen). RNA was preincubated with the oligo(dT) primer and dNTP at 65°C for 10 min followed by incubation at 42°C for 2 h; 1 μL of the cDNA samples was used for PCR amplification with 2 mM $MgCl_2$, 0.2 mM each dNTP, 1 unit of *Taq* DNA polymerase (Invitrogen), 1× PCR buffer, and 20 pmol of each primer for 30 cycles at an annealing temperature of 60°C.

Chimeric versions of the AGP18 coding sequence contain the cMyc or 6XHis antigenic epitopes (cMyc, EQKLISEEDL; 6XHis, HHHHHHA) introduced downstream of the N-terminal signal peptide were generated by double-joint PCR using cDNA as a template (Yu et al., 2004). All chimeric versions were analyzed in silico for potential secretion propensity using SignalP software (http://www.cbs.dtu.dk/services/SignalP/; Petersen et al., 2011), and the location of the signal peptide and GPI anchor were predicted using big-PI Predictor software (http://mendel.imp.ac.at/sat/gpi/gpi_server.html; Eisenhaber et al., 1999). Initially, a 114-bp fragment was amplified using primer combinations 18CDNA-S/SPMyc-18-AS or 18CDNA-S/SPHis-18-AS; this fragment includes the 5′-UTR, the AGP18 signal peptide, and the Tag fragment. An independent PCR was performed to amplify a 771-bp (cMyc) and a 762-bp (6XHis) fragment using primer pairs CDSMyc-18-S/18CDNA-AS or CDSHis-18-S/18CDNA-AS; this second fragment includes the Tag fragment (as an overlap to the 114-bp fragment), the AGP18 coding region backbone, and 3′-UTR. This construct configuration inserts the Tag fragment at position +84 of the endogenous sequence, taking as a reference the AGP18 transcription initiation site. Amplified products were purified and used as template in a joint PCR reaction. Fragments were reamplified using the primer pair 18CDNA-S/18CDNA-AS; an additional PCR fragment lacking the antigenic tag was amplified, cloned, and used as a control. To generate the CaMV35S-dependent overexpression constructs, resulting PCR products were cloned into pCR8 TOPO TA (Invitrogen) and used as donors in LR recombination (LR Clonase II; Invitrogen) with pMDC32 (Curtis and Grossniklaus, 2003); control vectors containing the CaMV35S promoter but no AGP18 sequences were also generated for subsequent transformation. To generate *proAGP18*-dependent endogenous expressing constructs, genomic regulatory regions previously described and characterized as transcriptional fusions were amplified using primer pairs 1S-GW-p18/1AS-GW-p18 and 2S-GW-p18/1AS-GW-p18; PCR products were cloned into pCR-TOPO 2.1 (Invitrogen), digested with *Asc*I and *Hin*dIII, and ligated into pMDC32 after eliminating the CaMV35S fragment, to generate pMDC-pAGP18$_{1622}$ and pMDC-pAGP18$_{1217}$ constructs; these pMDC constructs were used as Gateway destination vectors in recombination reactions with previously obtained AGP18 chimeric versions that contained either a cMyc or 6XHis tag. Seeds from T0 transformants were germinated in MS medium containing 50 μg mL^{-1} hygromycin B (Invitrogen). Developing siliques from all resistant lines were analyzed and scored for sterility defects. Selected lines were analyzed in T2 and confirmed by PCR amplification of the T-DNA insert. All primer sequences are described in Supplemental Table 4 online.

Histochemical Analysis

Inflorescences were fixed in FAA (10% formaldehyde, 5% acetic acid, and 50% ethanol) for 12 h and subsequently dehydrated in 70% ethanol. Gynoecia at different developing stages were dissected with hypodermic needles (1-mL insulin syringes), cleared in Herr's solution (phenol:chloral hydrate:85% lactic acid:xylene:clove oil in a 1:1:1:0.5:1 proportion), and observed with Nomarski optics using a DMR Leica microscope. Histochemical localization of GUS activity was performed by incubating dissected gynoecia in GUS staining solution (10 mM EDTA, 0.1% Triton X-100, 5 mM potassium ferrocyanide, 5 mM potassium ferricyanide, and 1 mg mL^{-1} 5-bromo-4-chloro-3-indolyl-β-D-glucuronic acid in 50 mM sodium phosphate buffer, pH 7.4) for 48 h at 37°C.

Immunolocalizations

Flowers at different developmental stages were fixed in 4% paraformaldehyde in PBS (10 mM KH_2PO_4 and 150 mM NaCl, pH 7) for 12 h at room temperature, gradually dehydrated in an ethanol series (10%), and

embedded in LR White Resin (Electron Microscopy Sciences). Sections (1.5 μm) were generated with an ultramicrotome (Leica Ultracut R) and placed on ProbeOnPlus (Fisher Biotech) slides. After washing twice with PBS, sections were blocked for 3 h with 5% BSA and 0.05% Tween 20 in PBS and incubated with the anti-Myc Tag antibody (Millipore, clone 4A6 1:50 in PBS containing 0.1% BSA) or JIM13 antibody, 1:10 in PBS and 0.1% BSA (Yates et al., 1996) for 6 h at room temperature. After washing with PBS, slides were incubated with Alexa Fluor 568 goat anti-mouse (Invitrogen) or with Texas Red-X goat anti-rat (Invitrogen) at a 1:100 dilution during 3 h at room temperature, washed with PBS, and counterstained with 1 μg mL^{-1} 4′,6-diamidino-2-phenylindole (Sigma-Aldrich). *proAGP18*$_{1622}$*:cMyc-AGP18-10* and *proAGP18*$_{1217}$*:cMyc-AGP18-12* were selected as reference lines. Slides were mounted with ProLong Gold antifade reagent (Invitrogen). Fluorescence was visualized using a Leica DM 6000B epifluorescence microscope using filter cubes N2.1 (excitation 515 to 560 nm; emission long-pass 590 nm) and UV filter A (excitation 340 to 380 nm; emission band-pass 470/40 nm). Images were acquired using Leica QWin Standard V3.4.0 (Leica Microsystems).

Accession Number

Sequence data from this article can be found in the Arabidopsis Genome Initiative or GenBank/EMBL databases under accession number At4g37450 (AGP18).

Supplemental Data

The following materials are available in the online version of this article.

Supplemental Figure 1. Pattern of GUS Expression Driven by the AGP18 Regulatory Region in Vegetative Tissues.

Supplemental Figure 2. Immunolocalization of AGP18 in Ovules of Wild-Type and *CaMV35S:AGP18* Transformant Lines Lacking a cMyc Tag.

Supplemental Figure 3. *Arabidopsis* Female Gametophyte Development in Wild-Type Ovules.

Supplemental Figure 4. Immunolocalization of Monoclonal Antibody JIM13 in Fully Differentiated Ovules.

Supplemental Table 1. Quantification of Transformant Lines Showing Reduced Fertility.

Supplemental Table 2. Quantification of Reduced Fertility in Selected Transformant Lines.

Supplemental Table 3. Cytological Analysis of Female Gametophyte Development in Fully Differentiated Ovules.

Supplemental Table 4. Primers Used in This Study.

ACKNOWLEDGMENTS

We thank Daphné Autran for critical reading and comments on the article, Javier Mendiola for technical help with transformation essays, two anonymous reviewers for helpful comments, and the genomic service at Langebio Cinvestav Irapuato for sequencing support. E.D.-A. was a recipient of a scholarship from Consejo Nacional de Ciencia y Tecnologia. Research was funded by grants from Consejo Nacional de Ciencia y Tecnologia, Consejo Estatal de Ciencia y Tecnologia de Guanajuato, and the Howard Hughes Medical Institute.

AUTHOR CONTRIBUTIONS

E.D.-A. performed the experiments. E.D.-A. and J.-P.V.-C. designed the research project, analyzed the results, and wrote the article.

Received October 11, 2012; revised February 28, 2013; accepted March 21, 2013; published April 9, 2013.

REFERENCES

Acosta-García, G., and Vielle-Calzada, J.P. (2004). A classical arabinogalactan protein is essential for the initiation of female gametogenesis in *Arabidopsis*. Plant Cell **16:** 2614–2628.

Agashe, B., Prasad, C.K., and Siddiqi, I. (2002). Identification and analysis of *DYAD*: A gene required for meiotic chromosome organisation and female meiotic progression in *Arabidopsis*. Development **129:** 3935–3943.

Bachelier, J.B., and Friedman, W.E. (2011). Female gamete competition in an ancient angiosperm lineage. Proc. Natl. Acad. Sci. USA **108:** 12360–12365.

Bajon, C., Horlow, C., Motamayor, J.C., Sauvanet, A., and Robert, D. (1999). Megasporogenesis in *Arabidopsis thaliana* L.: An ultrastructural study. Sex. Plant Reprod. **12:** 99–109.

Bechtold, N., Jaudeau, B., Jolivet, S., Maba, B., Vezon, D., Voisin, R., and Pelletier, G. (2000). The maternal chromosome set is the target of the T-DNA in the *in planta* transformation of *Arabidopsis thaliana*. Genetics **155:** 1875–1887.

Bell, P.R. (1996). Megaspore abortion: A consequence of selective apoptosis? Int. J. Plant Sci. **157:** 1–7.

Bencivenga, S., Colombo, L., and Masiero, S. (2011). Cross talk between the sporophyte and the megagametophyte during ovule development. Sex. Plant Reprod. **24:** 113–121.

Borner, G.H.H., Lilley, K.S., Stevens, T.J., and Dupree, P. (2003). Identification of glycosylphosphatidylinositol-anchored proteins in *Arabidopsis*. A proteomic and genomic analysis. Plant Physiol. **132:** 568–577.

Borner, G.H.H., Sherrier, D.J., Stevens, T.J., Arkin, I.T., and Dupree, P. (2002). Prediction of glycosylphosphatidylinositol-anchored proteins in *Arabidopsis*. A genomic analysis. Plant Physiol. **129:** 486–499.

Chen, C.G., Pu, Z.Y., Moritz, R.L., Simpson, R.J., Bacic, A., Clarke, A.E., and Mau, S.L. (1994). Molecular cloning of a gene encoding an arabinogalactan-protein from pear (*Pyrus communis*) cell suspension culture. Proc. Natl. Acad. Sci. USA **91:** 10305–10309.

Chen, J., et al. (2008). A triallelic system of S5 is a major regulator of the reproductive barrier and compatibility of indica-japonica hybrids in rice. Proc. Natl. Acad. Sci. USA **105:** 11436–11441.

Cheng, C.Y., Mathews, D.E., Eric Schaller, G., and Kieber, J.J. (2013). Cytokinin-dependent specification of the functional megaspore in the *Arabidopsis* female gametophyte. Plant J. **73:** 929–940.

Clough, S.J., and Bent, A.F. (1998). Floral dip: A simplified method for *Agrobacterium*-mediated transformation of *Arabidopsis thaliana*. Plant J. **16:** 735–743.

Coimbra, S., Almeida, J., Junqueira, V., Costa, M.L., and Pereira, L.G. (2007). Arabinogalactan proteins as molecular markers in *Arabidopsis thaliana* sexual reproduction. J. Exp. Bot. **58:** 4027–4035.

Couteau, F., Belzile, F., Horlow, C., Grandjean, O., Vezon, D., and Doutriaux, M.P. (1999). Random chromosome segregation without meiotic arrest in both male and female meiocytes of a *dmc1* mutant of *Arabidopsis*. Plant Cell **11:** 1623–1634.

Curtis, M.D., and Grossniklaus, U. (2003). A Gateway cloning vector set for high-throughput functional analysis of genes in planta. Plant Physiol. **133:** 462–469.

Curtis, M.J., Belcram, K., Bollmann, S.R., Tominey, C.M., Hoffman, P.D., Mercier, R., and Hays, J.B. (2009). Reciprocal chromosome translocation associated with TDNA-insertion mutation in *Arabidopsis*: Genetic and cytological analyses of consequences for gametophyte

development and for construction of doubly mutant lines. Planta **229:** 731–745.

Delker, C., Pöschl, Y., Raschke, A., Ullrich, K., Ettingshausen, S., Hauptmann, V., Grosse, I., and Quint, M. (2010). Natural variation of transcriptional auxin response networks in *Arabidopsis thaliana*. Plant Cell **22:** 2184–2200.

Desfeux, C., Clough, S.J., and Bent, A.F. (2000). Female reproductive tissues are the primary target of *Agrobacterium*-mediated transformation by the *Arabidopsis* floral-dip method. Plant Physiol. **123:** 895–904.

Du, H., Simpson, R.J., Moritz, R.L., Clarke, A.E., and Bacic, A. (1994). Isolation of the protein backbone of an arabinogalactan-protein from the styles of *Nicotiana alata* and characterization of a corresponding cDNA. Plant Cell **6:** 1643–1653.

Ebert, I., and Greilhuber, J. (2005). Developmental switch during embryo sac formation from a bisporic mode to the tetrasporic Fritillaria type in *Hyacinthoides vincentina* (Hoffmannsegg & Link) Rothm. (Hyacinthaceae). Acta Biol. Cracov. Bot. **47:** 179–184.

Eisenhaber, B., Bork, P., and Eisenhaber, F. (1999). Prediction of potential GPI-modification sites in proprotein sequences. J. Mol. Biol. **292:** 741–758.

Elliott, R.C., Betzner, A.S., Huttner, E., Oakes, M.P., Tucker, W.Q., Gerentes, D., Perez, P., and Smyth, D.R. (1996). *AINTEGUMENTA*, an *APETALA2*-like gene of *Arabidopsis* with pleiotropic roles in ovule development and floral organ growth. Plant Cell **8:** 155–168.

Ellis, M., Egelund, J., Schultz, C.J., and Bacic, A. (2010). Arabinogalactan-proteins: Key regulators at the cell surface? Plant Physiol. **153:** 403–419.

Estévez, J.M., Kieliszewski, M.J., Khitrov, N., and Somerville, C. (2006). Characterization of synthetic hydroxyproline-rich proteoglycans with arabinogalactan protein and extensin motifs in *Arabidopsis*. Plant Physiol. **142:** 458–470.

Friedman, W.E., and Ryerson, K.C. (2009). Reconstructing the ancestral female gametophyte of angiosperms: Insights from *Amborella* and other ancient lineages of flowering plants. Am. J. Bot. **96:** 129–143.

Hepworth, S.R., Valverde, F., Ravenscroft, D., Mouradov, A., and Coupland, G. (2002). Antagonistic regulation of flowering-time gene *SOC1* by CONSTANS and FLC via separate promoter motifs. EMBO J. **21:** 4327–4337.

Hruz, T., Laule, O., Szabo, G., Wessendorp, F., Bleuler, S., Oertle, L., Widmayer, P., Gruissem, W., and Zimmermann, P. (2008). Genevestigator v3: A reference expression database for the meta-analysis of transcriptomes. Adv. Bioinforma. **2008:** 420747.

Huang, B.-Q., Russell, S.D. (1992). Female germ unit: Organization, isolation and function. Int. Rev. Cytol. **140:** 233–293.

Jefferson, R.A., Kavanagh, T.A., and Bevan, M.W. (1987). GUS fusions: Beta-glucuronidase as a sensitive and versatile gene fusion marker in higher plants. EMBO J. **6:** 3901–3907.

Kapil, R.N., and Bhatnagar, A.K. (1981). Ultrastructure and biology of female gametophyte in flowering plants. Int. Rev. Cytol. **70:** 291–341.

Klimyuk, V.I., and Jones, J.D. (1997). *AtDMC1*, the *Arabidopsis* homologue of the yeast *DMC1* gene: Characterization, transposon-induced allelic variation and meiosis-associated expression. Plant J. **11:** 1–14.

Klucher, K.M., Chow, H., Reiser, L., and Fischer, R.L. (1996). The *AINTEGUMENTA* gene of *Arabidopsis* required for ovule and female gametophyte development is related to the floral homeotic gene *APETALA2*. Plant Cell **8:** 137–153.

Law, J.A., and Jacobsen, S.E. (2010). Establishing, maintaining and modifying DNA methylation patterns in plants and animals. Nat. Rev. Genet. **11:** 204–220.

Le Gourrierec, J., Li, Y.-F., and Zhou, D.-X. (1999). Transcriptional activation by *Arabidopsis* GT-1 may be through interaction with TFIIA-TBP-TATA complex. Plant J. **18:** 663–668.

Maheshwari, P. (1950). An Introduction to the Embryology of Angiosperms. (New York: McGraw-Hill).

McBride, K.E., and Summerfelt, K.R. (1990). Improved binary vectors for *Agrobacterium*-mediated plant transformation. Plant Mol. Biol. **14:** 269–276.

Misra, R.C. (1962). Contribution to the embryology of *Arabidopsis thalianum* (Gay and Monn.). Agra Univ. J. Res. **11:** 191–199.

Noher de Halac, I., and Harte, C. (1977). Different patterns of callose wall formation during megasporogenesis in 2 species of *Oenothera* (*Onagraceae*). Plant Syst. Evol. **127:** 23–38.

O'Connor, T.R., Dyreson, C., and Wyrick, J.J. (2005). Athena: A resource for rapid visualization and systematic analysis of *Arabidopsis* promoter sequences. Bioinformatics **21:** 4411–4413.

Olmedo-Monfil, V., Durán-Figueroa, N., Arteaga-Vázquez, M., Demesa-Arévalo, E., Autran, D., Grimanelli, D., Slotkin, R.K., Martienssen, R.A., and Vielle-Calzada, J.-P. (2010). Control of female gamete formation by a small RNA pathway in *Arabidopsis*. Nature **464:** 628–632.

Pagnussat, G.C., Alandete-Saez, M., Bowman, J.L., and Sundaresan, V. (2009). Auxin-dependent patterning and gamete specification in the *Arabidopsis* female gametophyte. Science **324:** 1684–1689.

Pandey, S., Wang, R.S., Wilson, L., Li, S., Zhao, Z., Gookin, T.E., Assmann, S.M., and Albert, R. (2010). Boolean modeling of transcriptome data reveals novel modes of heterotrimeric G-protein action. Mol. Syst. Biol. **6:** 372.

Pennell, R.I., Janniche, L., Kjellbom, P., Scofield, G.N., Peart, J.M., and Roberts, K. (1991). Developmental regulation of a plasma membrane arabinogalactan protein epitope in oilseed rape flowers. Plant Cell **3:** 1317–1326.

Pennell, R.I., Janniche, L., Scofield, G.N., Booij, H., de Vries, S.C., and Roberts, K. (1992). Identification of a transitional cell state in the developmental pathway to carrot somatic embryogenesis. J. Cell Biol. **119:** 1371–1380.

Pennell, R.I., and Roberts, K. (1990). Sexual development in the pea is presaged by altered expression of arabinogalactan protein. Nature **344:** 547–549.

Petersen, T.N., Brunak, S., von Heijne, G., and Nielsen, H. (2011). SignalP 4.0: Discriminating signal peptides from transmembrane regions. Nat. Methods **8:** 785–786.

Qiu, Y.L., Liu, R.S., Xie, C.T., Russell, S.D., and Tian, H.Q. (2008). Calcium changes during megasporogenesis and megaspore degeneration in lettuce (*Lactuca sativa* L.). Sex. Plant Reprod. **21:** 197–204.

Raj, A., Rifkin, S.A., Andersen, E., and van Oudenaarden, A. (2010). Variability in gene expression underlies incomplete penetrance. Nature **463:** 913–918.

Ray, S.M., Park, S.S., and Ray, A. (1997). Pollen tube guidance by the female gametophyte. Development **124:** 2489–2498.

Reiser, L., and Fischer, R.L. (1993). The ovule and the embryo sac. Plant Cell **5:** 1291–1301.

Robinson-Beers, K., Pruitt, R.E., and Gasser, C.S. (1992). Ovule development in wild-type *Arabidopsis* and two female-sterile mutants. Plant Cell **4:** 1237–1249.

Rodkiewicz, B. (1970). Callose in cell walls during megasporogenesis in angiosperms. Planta **93:** 39–47.

Russell, S.D. (1979). Fine structure of megagametophyte development in *Zea mays*. Can. J. Bot. **57:** 1093–1110.

Sánchez-León, N., et al. (2012). Transcriptional analysis of the *Arabidopsis* ovule by massively parallel signature sequencing. J. Exp. Bot. **63:** 3829–3842.

Schiefthaler, U., Balasubramanian, S., Sieber, P., Chevalier, D., Wisman, E., and Schneitz, K. (1999). Molecular analysis of *NOZZLE*, a gene involved in pattern formation and early sporogenesis during sex organ development in *Arabidopsis thaliana*. Proc. Natl. Acad. Sci. USA **96:** 11664–11669.

Schindelman, G., Morikami, A., Jung, J., Baskin, T.I., Carpita, N.C., Derbyshire, P., McCann, M.C., and Benfey, P.N. (2001). COBRA encodes a putative GPI-anchored protein, which is polarly localized and necessary for oriented cell expansion in *Arabidopsis*. Genes Dev. **15:** 1115–1127.

Schmidt, A., Wuest, S.E., Vijverberg, K., Baroux, C., Kleen, D., and Grossniklaus, U. (2011). Transcriptome analysis of the *Arabidopsis* megaspore mother cell uncovers the importance of RNA helicases for plant germline development. PLoS Biol. **9:** e1001155.

Schultz, C., Gilson, P., Oxley, D., Youl, J., and Bacic, A. (1998). GPI-anchors on arabinogalactan-proteins: implications for signalling in plants. Trends Plant Sci. **3:** 426–431.

Seifert, G.J., and Roberts, K. (2007). The biology of arabinogalactan proteins. Annu. Rev. Plant Biol. **58:** 137–161.

Sherrier, D.J., Prime, T.A., and Dupree, P. (1999). Glycosylphosphatidylinositol-anchored cell-surface proteins from *Arabidopsis*. Electrophoresis **20:** 2027–2035.

Skriver, K., Olsen, F.L., Rogers, J.C., and Mundy, J. (1991). Cis-acting DNA elements responsive to gibberellin and its antagonist abscisic acid. Proc. Natl. Acad. Sci. USA **88:** 7266–7270.

Stepanova, A.N., Robertson-Hoyt, J., Yun, J., Benavente, L.M., Xie, D.Y., Dolezal, K., Schlereth, A., Jürgens, G., and Alonso, J.M. (2008). *TAA1*-mediated auxin biosynthesis is essential for hormone crosstalk and plant development. Cell **133:** 177–191.

Sun, W., Zhao, Z.D., Hare, M.C., Kieliszewski, M.J., and Showalter, A.M. (2004). Tomato LeAGP-1 is a plasma membrane-bound, glycosylphosphatidylinositol-anchored arabinogalactan-protein. Physiol. Plant. **120:** 319–327.

Tan, L., Showalter, A.M., Egelund, J., Hernandez-Sanchez, A., Doblin, M.S., and Bacic, A. (2012). Arabinogalactan-proteins and the research challenges for these enigmatic plant cell surface proteoglycans. Front. Plant Sci. **3:** 140.

Tucker, M.R., and Koltunow, A.M. (2009). Sexual and asexual (apomictic) seed development in flowering plants: Molecular, morphological and evolutionary relationships. Funct. Plant Biol. **36:** 490–504.

Tucker, M.R., Okada, T., Hu, Y., Scholefield, A., Taylor, J.M., and Koltunow, A.M. (2012). Somatic small RNA pathways promote the mitotic events of megagametogenesis during female reproductive development in *Arabidopsis*. Development **139:** 1399–1404.

Ulmasov, T., Liu, Z.B., Hagen, G., and Guilfoyle, T.J. (1995). Composite structure of auxin response elements. Plant Cell **7:** 1611–1623.

Velasquez, S.M., et al. (2011). O-glycosylated cell wall proteins are essential in root hair growth. Science **332:** 1401–1403.

Webb, M.C., and Gunning, B.E.S. (1990). Embryo sac development in *Arabidopsis thaliana*. I. Megasporogenesis, including the microtubular cytoskeleton. Sex. Plant Reprod. **3:** 244–256.

Wuest, S.E., Vijverberg, K., Schmidt, A., Weiss, M., Gheyselinck, J., Lohr, M., Wellmer, F., Rahnenführer, J., von Mering, C., and Grossniklaus, U. (2010). *Arabidopsis* female gametophyte gene expression map reveals similarities between plant and animal gametes. Curr. Biol. **20:** 506–512.

Yamaguchi-Shinozaki, K., and Shinozaki, K. (1994). A novel *cis*-acting element in an *Arabidopsis* gene is involved in responsiveness to drought, low-temperature, or high-salt stress. Plant Cell **6:** 251–264.

Yang, J., and Showalter, A.M. (2007). Expression and localization of AtAGP18, a lysine-rich arabinogalactan-protein in *Arabidopsis*. Planta **226:** 169–179.

Yang, W.-C., Shi, D.-Q., and Chen, Y.-H. (2010). Female gametophyte development in flowering plants. Annu. Rev. Plant Biol. **61:** 89–108.

Yang, W.-C., and Sundaresan, V. (2000). Genetics of gametophyte biogenesis in *Arabidopsis*. Curr. Opin. Plant Biol. **3:** 53–57.

Yang, W.-C., Ye, D., Xu, J., and Sundaresan, V. (1999). The *SPOROCYTELESS* gene of *Arabidopsis* is required for initiation of sporogenesis and encodes a novel nuclear protein. Genes Dev. **13:** 2108–2117.

Yates, E.A., Valdor, J.-F., Haslam, S.M., Morris, H.R., Dell, A., Mackie, W., and Knox, J.P. (1996). Characterization of carbohydrate structural features recognized by anti-arabinogalactan-protein monoclonal antibodies. Glycobiology **6:** 131–139.

Youl, J.J., Bacic, A., and Oxley, D. (1998). Arabinogalactan-proteins from *Nicotiana alata* and *Pyrus communis* contain glycosylphosphatidylinositol membrane anchors. Proc. Natl. Acad. Sci. USA **95:** 7921–7926.

Yu, J.H., Hamari, Z., Han, K.H., Seo, J.A., Reyes-Domínguez, Y., and Scazzocchio, C. (2004). Double-joint PCR: A PCR-based molecular tool for gene manipulations in filamentous fungi. Fungal Genet. Biol. **41:** 973–981.

Zhang, Y., Yang, J., and Showalter, A.M. (2011a). AtAGP18 is localized at the plasma membrane and functions in plant growth and development. Planta **233:** 675–683.

Zhang, Y., Yang, J., and Showalter, A.M. (2011b). AtAGP18, a lysine-rich arabinogalactan protein in *Arabidopsis thaliana*, functions in plant growth and development as a putative co-receptor for signal transduction. Plant Signal. Behav. **6:** 855–857.